Three-Particle Coincidence of the Long Range Pseudorapidity Correlation in High Energy Nucleus-Nucleus Collisions

B. I. Abelev,[8] M. M. Aggarwal,[30] Z. Ahammed,[47] A. V. Alakhverdyants,[17] B. D. Anderson,[18] D. Arkhipkin,[3] G. S. Averichev,[17] J. Balewski,[22] O. Barannikova,[8] L. S. Barnby,[2] S. Baumgart,[52] D. R. Beavis,[3] R. Bellwied,[50] M. J. Betancourt,[22] R. R. Betts,[8] A. Bhasin,[16] A. K. Bhati,[30] H. Bichsel,[49] J. Bielcik,[10] J. Bielcikova,[11] B. Biritz,[6] L. C. Bland,[3] I. Bnzarov,[17] B. E. Bonner,[36] J. Bouchet,[18] E. Braidot,[27] A. V. Brandin,[25] A. Bridgeman,[1] E. Bruna,[52] S. Bueltmann,[29] T. P. Burton,[2] X. Z. Cai,[40] H. Caines,[52] M. Calderón de la Barca Sánchez,[5] O. Catu,[52] D. Cebra,[5] R. Cendejas,[6] M. C. Cervantes,[42] Z. Chajecki,[28] P. Chaloupka,[11] S. Chattopadhyay,[47] H. F. Chen,[38] J. H. Chen,[40] J. Y. Chen,[51] J. Cheng,[44] M. Cherney,[9] A. Chikanian,[52] K. E. Choi,[34] W. Christie,[3] P. Chung,[11] R. F. Clarke,[42] M. J. M. Codrington,[42] R. Corliss,[22] J. G. Cramer,[49] H. J. Crawford,[4] D. Das,[5] S. Dash,[13] A. Davila Leyva,[43] L. C. De Silva,[50] R. R. Debbe,[3] T. G. Dedovich,[17] M. DePhillips,[3] A. A. Derevschikov,[32] R. Derradi de Souza,[7] L. Didenko,[3] P. Djawotho,[42] S. M. Dogra,[16] X. Dong,[21] J. L. Drachenberg,[42] J. E. Draper,[5] J. C. Dunlop,[3] M. R. Dutta Mazumdar,[47] L. G. Efimov,[17] E. Elhalhuli,[2] M. Elnimr,[50] J. Engelage,[4] G. Eppley,[36] B. Erazmus,[41] M. Estienne,[41] L. Eun,[31] P. Fachini,[3] R. Fatemi,[19] J. Fedorisin,[17] R. G. Fersch,[19] P. Filip,[17] E. Finch,[52] V. Fine,[3] Y. Fisyak,[3] C. A. Gagliardi,[42] D. R. Gangadharan,[6] M. S. Ganti,[47] E. J. Garcia-Solis,[8] A. Geromitsos,[41] F. Geurts,[36] V. Ghazikhanian,[6] P. Ghosh,[47] Y. N. Gorbunov,[9] A. Gordon,[3] O. Grebenyuk,[21] D. Grosnick,[46] B. Grube,[34] S. M. Guertin,[6] A. Gupta,[16] N. Gupta,[16] W. Guryn,[3] B. Haag,[5] T. J. Hallman,[3] A. Hamed,[42] L-X. Han,[40] J. W. Harris,[52] J. P. Hays-Wehle,[22] M. Heinz,[52] S. Heppelmann,[31] A. Hirsch,[33] E. Hjort,[21] A. M. Hoffman,[22] G. W. Hoffmann,[43] D. J. Hofman,[8] R. S. Hollis,[8] H. Z. Huang,[6] T. J. Humanic,[28] L. Huo,[42] G. Igo,[6] A. Iordanova,[8] P. Jacobs,[21] W. W. Jacobs,[15] P. Jakl,[11] C. Jena,[13] F. Jin,[40] C. L. Jones,[22] P. G. Jones,[2] J. Joseph,[18] E. G. Judd,[4] S. Kabana,[41] K. Kajimoto,[43] K. Kang,[44] J. Kapitan,[11] K. Kauder,[8] D. Keane,[18] A. Kechechyan,[17] D. Kettler,[49] V. Yu. Khodyrev,[32] D. P. Kikola,[21] J. Kiryluk,[21] A. Kisiel,[48] A. G. Knospe,[52] A. Kocoloski,[22] D. D. Koetke,[46] T. Kollegger,[12] J. Konzer,[33] M. Kopytine,[18] I. Koralt,[29] W. Korsch,[19] L. Kotchenda,[25] V. Kouchpil,[11] P. Kravtsov,[25] V. I. Kravtsov,[32] K. Krueger,[1] M. Krus,[10] L. Kumar,[30] P. Kurnadi,[6] M. A. C. Lamont,[3] J. M. Landgraf,[3] S. LaPointe,[50] J. Lauret,[3] A. Lebedev,[3] R. Lednicky,[17] C-H. Lee,[34] J. H. Lee,[3] W. Leight,[22] M. J. LeVine,[3] C. Li,[38] L. Li,[43] N. Li,[51] W. Li,[40] X. Li,[33] X. Li,[39] Y. Li,[44] Z. Li,[51] G. Lin,[52] S. J. Lindenbaum,[26,*] M. A. Lisa,[28] F. Liu,[51] H. Liu,[5] J. Liu,[36] T. Ljubicic,[3] W. J. Llope,[36] R. S. Longacre,[3] W. A. Love,[3] Y. Lu,[38] T. Ludlam,[3] G. L. Ma,[40] Y. G. Ma,[40] D. P. Mahapatra,[13] R. Majka,[52] O. I. Mall,[5] L. K. Mangotra,[16] R. Manweiler,[46] S. Margetis,[18] C. Markert,[43] H. Masui,[21] H. S. Matis,[21] Yu. A. Matulenko,[32] D. McDonald,[36] T. S. McShane,[9] A. Meschanin,[32] R. Milner,[22] N. G. Minaev,[32] S. Mioduszewski,[42] A. Mischke,[27] M. K. Mitrovski,[12] B. Mohanty,[47] D. A. Morozov,[32] M. G. Munhoz,[37] B. K. Nandi,[14] C. Nattrass,[52] T. K. Nayak,[47] J. M. Nelson,[2] P. K. Netrakanti,[33] M. J. Ng,[4] L. V. Nogach,[32] S. B. Nurushev,[32] G. Odyniec,[21] A. Ogawa,[3] H. Okada,[3] V. Okorokov,[25] D. Olson,[21] M. Pachr,[10] B. S. Page,[15] S. K. Pal,[47] Y. Pandit,[18] Y. Panebratsev,[17] T. Pawlak,[48] T. Peitzmann,[27] V. Perevoztchikov,[3] C. Perkins,[4] W. Peryt,[48] S. C. Phatak,[13] P. Pile,[3] M. Planinic,[53] M. A. Ploskon,[21] J. Pluta,[48] D. Plyku,[29] N. Poljak,[53] A. M. Poskanzer,[21] B. V. K. S. Potukuchi,[16] C. B. Powell,[21] D. Prindle,[49] C. Pruneau,[50] N. K. Pruthi,[30] P. R. Pujahari,[14] J. Putschke,[52] R. Raniwala,[35] S. Raniwala,[35] R. L. Ray,[43] R. Redwine,[22] R. Reed,[5] J. M. Rehberg,[12] H. G. Ritter,[21] J. B. Roberts,[36] O. V. Rogachevskiy,[17] J. L. Romero,[5] A. Rose,[21] C. Roy,[41] L. Ruan,[3] R. Sahoo,[41] S. Sakai,[6] I. Sakrejda,[21] T. Sakuma,[22] S. Salur,[5] J. Sandweiss,[52] E. Sangaline,[5] J. Schambach,[43] R. P. Scharenberg,[33] N. Schmitz,[23] T. R. Schuster,[12] J. Seele,[22] J. Seger,[9] I. Selyuzhenkov,[15] P. Seyboth,[23] E. Shahaliev,[17] M. Shao,[38] M. Sharma,[50] S. S. Shi,[51] E. P. Sichtermann,[21] F. Simon,[23] R. N. Singaraju,[47] M. J. Skoby,[33] N. Smirnov,[52] P. Sorensen,[3] J. Sowinski,[15] H. M. Spinka,[1] B. Srivastava,[33] T. D. S. Stanislaus,[46] D. Staszak,[6] J. R. Stevens,[15] R. Stock,[12] M. Strikhanov,[25] B. Stringfellow,[33] A. A. P. Suaide,[37] M. C. Suarez,[8] N. L. Subba,[18] M. Sumbera,[11] X. M. Sun,[21] Y. Sun,[38] Z. Sun,[20] B. Surrow,[22] T. J. M. Symons,[21] A. Szanto de Toledo,[37] J. Takahashi,[7] A. H. Tang,[3] Z. Tang,[38] L. H. Tarini,[50] T. Tarnowsky,[24] D. Thein,[43] J. H. Thomas,[21] J. Tian,[40] A. R. Timmins,[50] S. Timoshenko,[25] D. Tlusty,[11] M. Tokarev,[17] V. N. Tram,[21] S. Trentalange,[6] R. E. Tribble,[42] O. D. Tsai,[6] J. Ulery,[33] T. Ullrich,[3] D. G. Underwood,[1] G. Van Buren,[3] G. van Nieuwenhuizen,[22] M. van Leeuwen,[27] J. A. Vanfossen, Jr.,[18] R. Varma,[14] G. M. S. Vasconcelos,[7] A. N. Vasiliev,[32] F. Videbæk,[3] Y. P. Viyogi,[47] S. Vokal,[17] M. Wada,[43] M. Walker,[22] F. Wang,[33] G. Wang,[6] H. Wang,[24] J. S. Wang,[20] Q. Wang,[33] X. Wang,[44] X. L. Wang,[38] Y. Wang,[44] G. Webb,[19] J. C. Webb,[46] G. D. Westfall,[24] C. Whitten, Jr.,[6] H. Wieman,[21] E. Wingfield,[43] S. W. Wissink,[15] R. Witt,[45] Y. Wu,[51] W. Xie,[33] N. Xu,[21] Q. H. Xu,[39] W. Xu,[6] Y. Xu,[38] Z. Xu,[3] L. Xue,[40] Y. Yang,[20] P. Yepes,[36] K. Yip,[3] I-K. Yoo,[34] Q. Yue,[44] M. Zawisza,[48] H. Zbroszczyk,[48] W. Zhan,[20] S. Zhang,[40] W. M. Zhang,[18] X. P. Zhang,[21] Y. Zhang,[21] Z. P. Zhang,[38] J. Zhao,[40] C. Zhong,[40]

J. Zhou,[36] W. Zhou,[39] X. Zhu,[44] Y-H. Zhu,[40] R. Zoulkarneev,[17] and Y. Zoulkarneeva[17]

(STAR Collaboration)

[1]*Argonne National Laboratory, Argonne, Illinois 60439, USA*
[2]*University of Birmingham, Birmingham, United Kingdom*
[3]*Brookhaven National Laboratory, Upton, New York 11973, USA*
[4]*University of California, Berkeley, California 94720, USA*
[5]*University of California, Davis, California 95616, USA*
[6]*University of California, Los Angeles, California 90095, USA*
[7]*Universidade Estadual de Campinas, Sao Paulo, Brazil*
[8]*University of Illinois at Chicago, Chicago, Illinois 60607, USA*
[9]*Creighton University, Omaha, Nebraska 68178, USA*
[10]*Czech Technical University in Prague, FNSPE, Prague, 115 19, Czech Republic*
[11]*Nuclear Physics Institute AS CR, 250 68 Řež/Prague, Czech Republic*
[12]*University of Frankfurt, Frankfurt, Germany*
[13]*Institute of Physics, Bhubaneswar 751005, India*
[14]*Indian Institute of Technology, Mumbai, India*
[15]*Indiana University, Bloomington, Indiana 47408, USA*
[16]*University of Jammu, Jammu 180001, India*
[17]*Joint Institute for Nuclear Research, Dubna, 141 980, Russia*
[18]*Kent State University, Kent, Ohio 44242, USA*
[19]*University of Kentucky, Lexington, Kentucky, 40506-0055, USA*
[20]*Institute of Modern Physics, Lanzhou, China*
[21]*Lawrence Berkeley National Laboratory, Berkeley, California 94720, USA*
[22]*Massachusetts Institute of Technology, Cambridge, Massachusetts 02139-4307, USA*
[23]*Max-Planck-Institut für Physik, Munich, Germany*
[24]*Michigan State University, East Lansing, Michigan 48824, USA*
[25]*Moscow Engineering Physics Institute, Moscow Russia*
[26]*City College of New York, New York City, New York 10031, USA*
[27]*NIKHEF and Utrecht University, Amsterdam, The Netherlands*
[28]*Ohio State University, Columbus, Ohio 43210, USA*
[29]*Old Dominion University, Norfolk, Virginia, 23529, USA*
[30]*Panjab University, Chandigarh 160014, India*
[31]*Pennsylvania State University, University Park, Pennsylvania 16802, USA*
[32]*Institute of High Energy Physics, Protvino, Russia*
[33]*Purdue University, West Lafayette, Indiana 47907, USA*
[34]*Pusan National University, Pusan, Republic of Korea*
[35]*University of Rajasthan, Jaipur 302004, India*
[36]*Rice University, Houston, Texas 77251, USA*
[37]*Universidade de Sao Paulo, Sao Paulo, Brazil*
[38]*University of Science & Technology of China, Hefei 230026, China*
[39]*Shandong University, Jinan, Shandong 250100, China*
[40]*Shanghai Institute of Applied Physics, Shanghai 201800, China*
[41]*SUBATECH, Nantes, France*
[42]*Texas A&M University, College Station, Texas 77843, USA*
[43]*University of Texas, Austin, Texas 78712, USA*
[44]*Tsinghua University, Beijing 100084, China*
[45]*United States Naval Academy, Annapolis, Maryland 21402, USA*
[46]*Valparaiso University, Valparaiso, Indiana 46383, USA*
[47]*Variable Energy Cyclotron Centre, Kolkata 700064, India*
[48]*Warsaw University of Technology, Warsaw, Poland*
[49]*University of Washington, Seattle, Washington 98195, USA*
[50]*Wayne State University, Detroit, Michigan 48201, USA*
[51]*Institute of Particle Physics, CCNU (HZNU), Wuhan 430079, China*
[52]*Yale University, New Haven, Connecticut 06520, USA*
[53]*University of Zagreb, Zagreb, HR-10002, Croatia*
(Received 8 February 2010; published 8 July 2010)

We report the first three-particle coincidence measurement in pseudorapidity ($\Delta\eta$) between a high transverse momentum ($p_\perp$) trigger particle and two lower $p_\perp$ associated particles within azimuth $|\Delta\phi| < 0.7$ in $\sqrt{s_{\rm NN}} = 200$ GeV d + Au and Au + Au collisions. Charge ordering properties are exploited to separate the jetlike component and the ridge (long range $\Delta\eta$ correlation). The results indicate that the correlation of ridge particles are uniform not only with respect to the trigger particle but also between themselves event by event in our measured $\Delta\eta$. In addition, the production of the ridge appears to be uncorrelated to the presence of the narrow jetlike component.

DOI: 10.1103/PhysRevLett.105.022301 PACS numbers: 25.75.Bh, 25.75.Nq

Di-hadron coincidence measurements provide a powerful tool to study the properties of the medium created in ultrarelativistic heavy-ion collisions. The observation of the long range pseudorapidity correlation in central Au + Au collisions [1], called the ridge [2], where hadrons are correlated with a high transverse momentum ($p_\perp$) trigger particle in azimuth ($\Delta\phi \sim 0$) but extended to large relative pseudorapidity ($\Delta\eta$), has generated great interest. Various theoretical models are proposed to explain this phenomenon, including (i) longitudinal flow push [3], (ii) broadening of quenched jets in turbulent color fields [4], (iii) recombination between thermal and shower partons [5], (iv) elastic collisions between hard and medium partons (momentum kick) [6], and (v) particle excess due to QCD bremsstrahlung or color flux tube fluctuations focused by transverse radial flow [7–11]. Models (i)–(iv) attribute the ridge to jet-medium interactions: particles from jet fragmentation in vacuum result in a peak at $\Delta\eta \sim 0$ and those affected by the medium are diffused broadly in $\Delta\eta$ forming the ridge. Model (v) attributes the ridge to the medium itself, and its correlation with high-$p_\perp$ particles is due to the transverse radial flow.

Despite very different physics mechanisms, all models [3–11] give qualitatively similar distributions of correlated hadrons with a high-$p_\perp$ trigger particle. Some of these model ambiguities can be lifted by three-particle coincidence measurements. We analyze the hadron pair densities from three-particle coincidence measurements in ($\Delta\eta_1$, $\Delta\eta_2$), the pseudorapidity differences between two associated particles and a trigger particle. We exploit charge combinations in an attempt to separate the jetlike and ridge components and study their distributions, without assuming the $\Delta\eta$ shape of the ridge. Jet fragmentation in vacuum should give a peak at $(\Delta\eta_1, \Delta\eta_2) \sim (0, 0)$, while particles from the ridge would produce structures that depend on its physics mechanism. Correlation between particles from jet fragmentation and the ridge would generate horizontal or vertical stripes ($\Delta\eta_1 \sim 0$ or $\Delta\eta_2 \sim 0$) in the three-particle coincidence measurement.

Results are reported for minimum bias d + Au, peripheral 40%–80% and central 0%–12% Au + Au collisions at $\sqrt{s_{\rm NN}} = 200$ GeV from the STAR experiment [12]. The 40%–80% data are from the minimum bias sample, and the 0%–12% data are triggered by the zero degree calorimeters (ZDC) in combination with the central trigger barrel (CTB). This analysis uses 6.5×10^6 d + Au events taken in 2003, and 6.0×10^6 peripheral and 1.9×10^7 central Au + Au events taken in 2004. The data are analyzed in finer centrality bins for Au + Au collisions [13] and are combined for better statistics.

The reconstructed event vertex is restricted within $|z_{\rm vtx}| < 30$ cm along the beam line from the center of the STAR time projection chamber (TPC) [14], which sits in a uniform 0.5 T magnetic field with full azimuthal coverage. The data were taken with both magnetic field polarities. The trigger and associated particles are restricted to $|\eta| < 1 (|\Delta\eta| < 2)$ and their $p_\perp$ ranges are $3 < p_\perp^{(t)} < 10$ GeV/c and $1 < p_\perp^{(a)} < 3$ GeV/c, respectively. The correlated single and pair densities with trigger particle are corrected for the centrality-, $p_\perp$-, ϕ-dependent reconstruction efficiency for associated particles and the ϕ-dependent efficiency for trigger particles, and are normalized per corrected trigger particle.

Because of the high TPC occupancy of Au + Au events, track pairs close in η and ϕ can be merged and reconstructed as single tracks. This results in deficits in pair density at $\Delta\eta \sim 0$ and at small, but nonzero, $\Delta\phi$ whose value depends on $p_\perp$, charge combination and magnetic field polarity. To reduce this effect, we apply cuts to exclude close track pairs in real and mixed events. Losses due to those cuts are compensated for by the acceptance correction obtained from mixed events. To ensure the mixed events have similar characteristics as the real events, we mix events from the same centrality bin without requiring a trigger particle and with the same magnetic field polarity and nearly identical $z_{\rm vtx}$ position, referred to hereon as inclusive events.

Figure 1(a) shows the hadron $\Delta\phi$ distributions relative to the trigger particle in 0%–12% Au + Au collisions. Also shown is the background $B(\Delta\phi) = aF(\Delta\phi) \times \int_{-2}^{2} B_{\rm inc}(\Delta\eta, \Delta\phi) d\Delta\eta$ where $B_{\rm inc}$ is constructed by mixing a trigger particle with associated particles from a different and inclusive event. The flow contribution

$$F(\Delta\phi) = 1 + 2v_2^{(t)}v_2^{(a)}\cos(2\Delta\phi) + 2v_4^{(t)}v_4^{(a)}\cos(4\Delta\phi) \quad (1)$$

is added to mixed events using the measured, η independent, v_2 [15] and a parameterization of $v_4 = 1.15v_2^2$ [13]. A normalization factor, a, is applied to match the distribu-

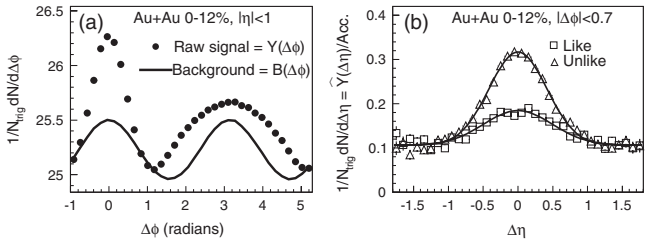

FIG. 1. Correlated hadron distribution in (a) $\Delta\phi$ ($|\eta| < 1$), and (b) $\Delta\eta$ ($|\Delta\phi| < 0.7$) with a high-$p_\perp$ trigger particle in 0%–12% Au + Au collisions for $3 < p_\perp^{(t)} < 10$ GeV/c and $1 < p_\perp^{(a)} < 3$ GeV/c. The ZYA1-normalized flow background is shown in (a) by the curve. The $\Delta\eta$ distributions in (b) are background subtracted and corrected for $\Delta\eta$ acceptance, and are for like- and unlike-sign pairs separately. The curves in (b) are Gaussian fits. Errors are statistical.

tion in $0.8 < |\Delta\phi| < 1.2$, assuming zero yield at $|\Delta\phi| \sim 1$ radian (ZYA1) [1].

The nearside ($|\Delta\phi| < 0.7$) correlated hadron yield in $\Delta\eta$ is $\hat{Y}(\Delta\eta) = Y(\Delta\eta) - B(\Delta\eta)$, where $Y(\Delta\eta)$ and $B(\Delta\eta) = a\int_{-0.7}^{0.7} B_{\rm inc}(\Delta\eta, \Delta\phi)F(\Delta\phi)d\Delta\phi$ are the signal and background distributions, respectively. Figure 1(b) shows the $\hat{Y}(\Delta\eta)$ distribution, after two-particle $\Delta\eta$ acceptance correction, for the like- and unlike-sign trigger-correlated particle pairs. Jetlike peaks at $\Delta\eta \sim 0$ are observed, atop a broad, charge-independent pedestal (the ridge). A Gaussian fit to the peak yields 0.49 ± 0.03 for the like-sign and 0.41 ± 0.01 for the unlike-sign pairs in $\Delta\eta$.

All triplets of one trigger particle and two associated particles from the same event within $|\Delta\phi_{1,2}| < 0.7$ are analyzed. Combinatorial background B_1 (or B_2) arises where only one (or neither) of the two associated particles is correlated with the trigger particle besides flow correlation [16]. The former cannot be readily obtained from the product of the event averaged $\hat{Y}(\Delta\eta)$ and $B(\Delta\eta)$, because of the varying $\Delta\eta$ acceptance from event to event. Instead, we construct B_1 by mixing trigger-associated pairs from the real event with a particle from a different and inclusive event, namely,

$$\begin{aligned} B_1 = &[aY(\Delta\eta_1)B_{\rm inc}(\Delta\eta_2)\langle F^{(t,2)}(\Delta\phi_2) + F^{(1,2)}(\Delta\phi_1 - \Delta\phi_2) \\ &+ F' - 1\rangle] + [(1 \leftrightarrow 2)] \\ &- [2a^2 B_{\rm inc}(\Delta\eta_1)B_{\rm inc}(\Delta\eta_2)\langle F^{(t,1)}(\Delta\phi_1) + F^{(t,2)}(\Delta\phi_2) \\ &+ F^{(1,2)}(\Delta\phi_1 - \Delta\phi_2) + F' - 2\rangle], \end{aligned} \tag{2}$$

where $B_{\rm inc}(\Delta\eta) = \int_{-0.7}^{0.7} B_{\rm inc}(\Delta\eta, \Delta\phi)d\Delta\phi$. The last term in Eq. (2) is constructed by mixing the trigger particle with two different inclusive events to remove the uncorrelated part in the first two terms, and

$$\begin{aligned} F' = &2v_2^{(t)}v_2^{(1)}v_4^{(2)}\cos(2\Delta\phi_1 - 4\Delta\phi_2) \\ &+ 2v_2^{(t)}v_2^{(2)}v_4^{(1)}\cos(4\Delta\phi_1 - 2\Delta\phi_2) \\ &+ 2v_2^{(1)}v_2^{(2)}v_4^{(t)}\cos(2\Delta\phi_1 + 2\Delta\phi_2). \end{aligned} \tag{3}$$

The flow terms [16] in $\langle\ldots\rangle$ are added in because they are lost in the event-mixing; their averages are taken within $|\Delta\phi_{1,2}| < 0.7$. The superscripts represent the v_2 and v_4 for trigger and associated particles. To increase statistics, we mix each trigger particle with ten different inclusive events.

The second background (B_2) is constructed by mixing a trigger particle with associated particle pairs from inclusive events thereby preserving all correlations between the two associated particles (denoted by $\otimes$) [16]:

$$\begin{aligned} B_2 = &a^2 b[B_{\rm inc}(\Delta\eta_1) \otimes B_{\rm inc}(\Delta\eta_2)]\langle F^{(t,1)}(\Delta\phi_1) \\ &+ F^{(t,2)}(\Delta\phi_2) + F' - 1\rangle. \end{aligned} \tag{4}$$

The factor $a^2 b$ scales the number of associated hadron pairs in the inclusive event to that in the background underlying the triggered event: $b = (\langle N(N-1)\rangle/\langle N\rangle^2)_{\rm bkgd}/(\langle N(N-1)\rangle/\langle N\rangle^2)_{\rm inc}$, where N denotes the associated hadron multiplicity [16]. If the associated hadron multiplicity distributions in both the inclusive event and the background are Poissonian, or deviate from it equally, then $b = 1$. We obtain b as follows. We scale the correlated hadron $\Delta\eta$ distribution such that there would be no ridge in $1.0 < |\Delta\eta| < 1.8$, and this gives a new value for a. We repeat our analysis with this new a, and obtain b by requiring the average correlated hadron pair density in $1.0 < |\Delta\eta_{1,2}| < 1.8$ be zero. We use the obtained b with the default ZYA1 a to obtain the final three-particle coincidence signal. The assumption in this procedure is

$$[\langle N(N-1)\rangle/\langle N\rangle^2]_{\rm bkgd} = [\langle N(N-1)\rangle/\langle N\rangle^2]_{\rm bkgd+ridge}, \tag{5}$$

and is reasonable gauged from multiplicity distributions of inclusive and triggered events. The background-subtracted correlated pair density is corrected for three-particle $\Delta\eta$-$\Delta\eta$ acceptance, which is obtained from event-mixing of a trigger particle with associated particles from two different inclusive events. We use ten pairs of inclusive events for each trigger particle in the mixing.

The main sources of systematic uncertainty in our results are those in a, b, and v_2. These uncertainties are mostly correlated, and, therefore have an insignificant effect on the shapes of our correlated density distributions. The a and b values for 0%–12% Au + Au collisions are $0.9986^{+0.0020}_{-0.0006}$(syst) and $0.99982^{+0.000\,02}_{-0.000\,05}$(syst), respectively. The uncertainty on a is estimated by using the normalization ranges of $0.9 < \Delta\phi < 1.1$ and $0.7 < \Delta\phi < 1.3$. That on b is estimated by using the normalization ranges of $1.2 < |\Delta\eta| < 1.8$ and $0.6 < |\Delta\eta| < 1.2$. We note that the ridge is defined under the assumption of ZYA1 in $\Delta\phi$, by

the factor a. Deviations of a from this assumption are not included in our systematic uncertainties. Such deviations (e.g. three-particle ZYAM [13]) do not introduce significant change to the shape of the ridge.

The v_2 systematic range used in our analysis is given by those from the modified reaction plane and four-particle cumulant methods [1] and their average is used as our nominal v_2. The uncertainty in v_4 is estimated by varying the v_4 by $\pm 20\%$. An additional systematic uncertainty arises from possible correlation of the ridge with the reaction plane which is not included in Eq. (2). The estimated uncertainty from this source and that from v_2 and v_4 are added in quadrature and referred to generally as flow uncertainty.

Figures 2(a)–2(c) show the background-subtracted and $\Delta\eta$-$\Delta\eta$ acceptance corrected charge-independent (referred to as AAT) correlated hadron pair density ($\hat{P}$) for minimum bias d + Au, 40%–80% and 0%–12% Au + Au collisions, respectively. The d + Au and 40%–80% Au + Au results show a peak at $(\Delta\eta_1, \Delta\eta_2) \sim (0, 0)$, consistent with jet fragmentation in vacuum. A similar peak is also contained within 0%–12% Au + Au collisions, but it is atop an overall pedestal. This pedestal is composed of the ridge particle pairs, and does not seem to have other structures in $(\Delta\eta_1, \Delta\eta_2)$. To see this quantitatively, Fig. 3(a) shows the average $\langle\hat{P}\rangle$ for AAT as a function of $R = \sqrt{\Delta\eta_1^2 + \Delta\eta_2^2}$. The average density is peaked at $R \sim 0$ and decreases with R for all systems. For d + Au and 40%–80% Au + Au collisions the average density at $R > 1$ is consistent with zero, indicating no ridge contribution. On the other hand, in 0%–12% Au + Au collisions, the average density drops more slowly and becomes approximately constant above $R > 1$, indicating the presence of the ridge.

Jet fragmentation has a charge ordering property, as shown at $|\Delta\eta| \sim 0$ in Fig. 1(b). The probability to fragment into three same-sign hadrons at our energy scale is small [17,18]. We analyze our data with same-sign triplets $(A^{\pm}A^{\pm}T^{\pm})$ and with a same-sign associated pair and an opposite-sign trigger particle $(A^{\pm}A^{\pm}T^{\mp})$. Figure. 3(b) shows the $A^{\pm}A^{\pm}T^{\pm}$ results in d + Au and 40%–80% Au + Au. Indeed, the $A^{\pm}A^{\pm}T^{\pm}$ signals are small indicating small jetlike contributions. Also shown are $A^{\pm}A^{\pm}T^{\pm}$ and $A^{\pm}A^{\pm}T^{\mp}$ in 0%–12% Au + Au collisions. No jetlike contribution is apparent in $A^{\pm}A^{\pm}T^{\pm}$. The contribution from other charge combinations, namely $A^{\pm}A^{\mp}T^{\pm}$, are simply the difference between AAT in Fig. 3(a) and $(A^{\pm}A^{\pm}T^{\pm} + A^{\pm}A^{\pm}T^{\mp})$ in Fig. 3(b). We found this to be equal to twice the $A^{\pm}A^{\pm}T^{\mp}$ contribution within errors.

The ridge is similar for like- and unlike-sign trigger-associated pairs at $|\Delta\eta| > 0.7$ as shown in Fig. 1(b); thus, we expect the ridge contributions in the correlated pair density to be the same in all charge combinations. We verified this for large $\Delta\eta$ correlated pair densities within our current statistics, as can be seen from Fig. 3(b). Therefore, 4 times $A^{\pm}A^{\pm}T^{\pm}$ contains the total ridge particle pair density ($\hat{P}_{rr}$). The remaining signal ($AAT - 4 \times A^{\pm}A^{\pm}T^{\pm}$, where systematic uncertainties are correlated) contain the total jetlike pairs ($\hat{P}_{jj}$). Figure. 4(a) shows the R dependence of the average ridge and jetlike signals. The systematic uncertainties due to possible contamination of jet-jet pairs in $A^{\pm}A^{\pm}T^{\pm}$ [see the d + Au data in Fig. 3(b)] are not shown, but included in the quoted uncertainties in the fitted σ's below.

Both the jetlike and ridge signals should contain cross pairs of a jetlike and a ridge particle ($\hat{P}_{jr}$), larger in the former because of the larger unlike-sign contribution [see Fig. 1(b)]. We average the jetlike pair densities in $|\Delta\eta_{1(\text{or }2)}| < 0.7$ and $|\Delta\eta_{2(\text{or }1)}| > 0.7$ region and obtain -0.004 ± 0.025, the upper estimate of $\langle\hat{P}_{jr}\rangle/2$. The correlated jet-jet and ridge-ridge pairs, $\sqrt{\langle\hat{P}_{jj}\rangle\langle\hat{P}_{rr}\rangle} = \sqrt{(0.077 \pm 0.026) \times (0.114 \pm 0.039)} = 0.094 \pm 0.023$, where the averages are taken with $|\Delta\eta_{1,2}| < 0.7$ and $|\Delta\eta_{1,2}| > 0.7$, respectively. The comparison between $\langle\hat{P}_{jr}\rangle$ and $\sqrt{\langle\hat{P}_{jj}\rangle\langle\hat{P}_{rr}\rangle}$ (whose systematic uncertainties are strongly correlated) suggests that the production of the ridge and the jetlike particles may be uncorrelated.

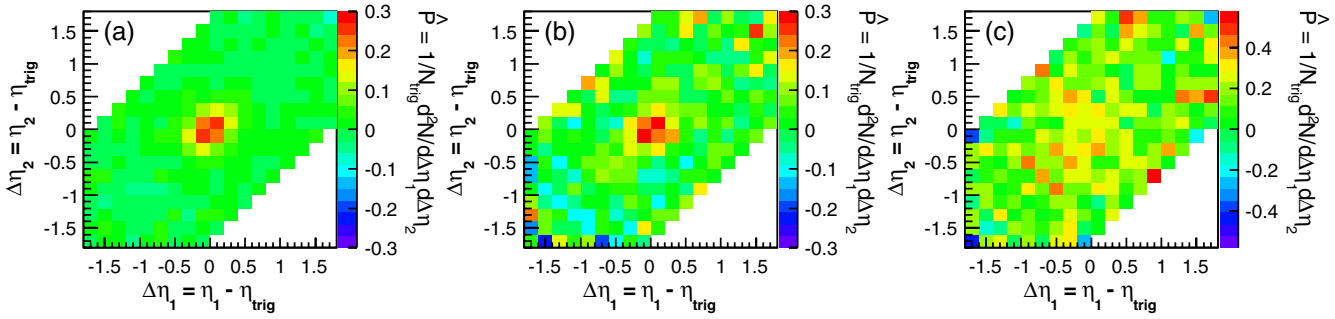

FIG. 2 (color online). Background-subtracted charge-independent (AAT) correlated hadron pair density in (a) minimum bias d + Au, (b) 40%–80% Au + Au, and (c) 0%–12% Au + Au collisions for $3 < p_{\perp}^{>(t)} < 10$ GeV/c and $1 < p_{\perp}^{(a)} < 3$ GeV/c. The results are for near-side correlated hadrons within $|\Delta\phi_{1,2}| < 0.7$, and corrected for the three-particle $\Delta\eta$-$\Delta\eta$ acceptance. Statistical errors at $(\Delta\eta_1, \Delta\eta_2) \sim (0, 0)$ are approximately 0.018, 0.054, 0.084 for d + Au, 40%–80% and 0%–12% Au + Au, respectively.

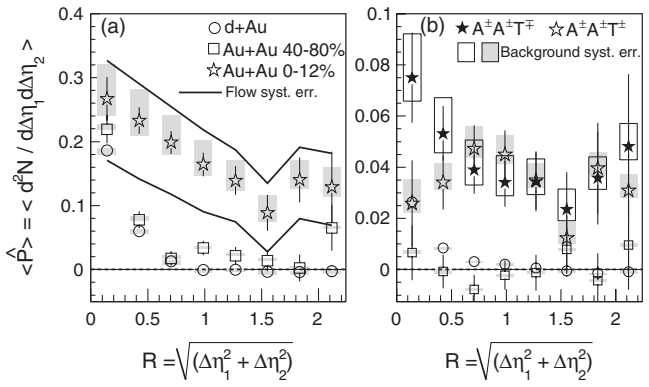

FIG. 3. The average correlated hadron pair density per trigger particle as a function of R (a) for all charges, and (b) for same-sign triplets ($A^{\pm}A^{\pm}T^{\pm}$) in all systems and for same-sign associated particles with an opposite-sign trigger particle $A^{\pm}A^{\pm}T^{\mp}$) in 0%–12% Au + Au collisions.

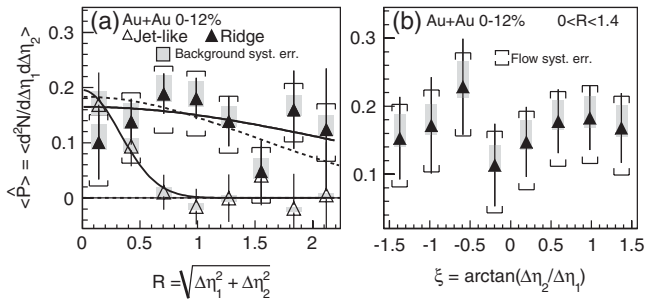

FIG. 4. The average correlated hadron pair density per trigger particle in 0%–12% Au + Au collisions (a) for the jetlike and ridge components as a function of R, and (b) for the ridge as a function of ξ within $R < 1.4$. The solid curves are Gaussian fits. The dashed curve is a Gaussian fit with a fixed $\sigma = 1.48$ (see text) to the ridge data.

Because $\langle \hat{P}_{jr} \rangle \sim 0$, the ridge and jetlike signals shown in Fig. 4(a) are essentially $\langle \hat{P}_{rr} \rangle$ and $\langle \hat{P}_{jj} \rangle$. The ridge pair density $\langle \hat{P}_{rr} \rangle$ is consistent with a constant $0.15 \pm 0.02(\text{stat}) \pm 0.03(\text{syst})$ ($\chi^2/\text{ndf} = 6.2/7$). Gaussian fits indicate a best fit value $\sigma = 2.30^{+1.21}_{-0.01}(\text{syst})$ ($\chi^2/\text{ndf} = 5.1/6$), and $\sigma > 1.48^{+0.33}_{-0.06}(\text{syst})$ with 84% confidence level. On the other hand, the jet pair density is narrow with a Gaussian $\sigma = 0.33^{+0.09}_{-0.07}(\text{stat})^{+0.01}_{-0.02}(\text{syst})$ ($\chi^2/\text{ndf} = 1.1/6$), comparing well to those from the correlated single hadron density.

In order to investigate possible structures in the ridge, we show in Fig. 4(b) the average ridge particle pair density as a function of $\xi = \arctan(\Delta\eta_2/\Delta\eta_1)$ within $R < 1.4$. The data are consistent with a uniform distribution in ξ ($\chi^2/\text{ndf} = 1.8/7$). This suggests that the ridge particles are uncorrelated in $\Delta\eta$ not only with the trigger particle but also between themselves. In other words, the ridge appears to be uniform in $\Delta\eta$ event by event.

Our data qualitatively distinguish between some of the ridge models. (i) Longitudinal flow [3] would push correlated particles in one direction yielding a diagonal excess in $\Delta\eta$-$\Delta\eta$, disfavored by the present data. (ii) Turbulent color fields [4] would generate a broad ridge in $\Delta\eta$, which may however still be too narrow to reconcile with the width of our ridge pair density distribution. (iii) Recombination between thermal and shower partons [5] should produce horizontal and vertical stripes in correlated pair density distribution which is disfavored by the data, and it does not have a mechanism for long range $\Delta\eta$ correlations. (iv) The momentum kick model incorporates a broad ridge as input, but it should produce a much larger ridge on the away-side than on the near-side which is not supported by data [19], and also may not describe other data such as the reaction plane dependence of the ridge in di-hadron correlations [20]. (v) QCD bremsstrahlung [7,8] or color flux tube fluctuations [9–11] would yield a structureless pair density [10] for the ridge as observed in our data; however, the correlations between jetlike particles and ridge, as expected from these models, are not observed with our present sensitivity. Clearly, more quantitative model calculations are needed to compare to the data reported here and elsewhere [1,2,20] to further our understanding of the ridge.

In summary, we have presented the first three-particle coincidence measurement in $\Delta\eta$-$\Delta\eta$ in minimum bias d + Au, 40%–80% and 0%–12% Au + Au collisions at $\sqrt{s_{\text{NN}}} = 200$ GeV. The $p_\perp$ ranges are $3 < p_\perp^{(t)} < 10\ \text{GeV}/c$ for the trigger particle and $1 < p_\perp^{(a)} < 3\ \text{GeV}/c$ for both associated particles. A correlated hadron pair density peak at $(\Delta\eta_1, \Delta\eta_2) \sim (0, 0)$, characteristic of jet fragmentation, is observed in all systems. This peak sits atop a broad pedestal in 0%–12% Au + Au collisions, which is composed of particle pairs from the ridge. We have exploited the charge ordering properties to separate the jetlike and ridge components. We found that same-sign associated pairs correlated with a same-sign trigger particle are dominated by the ridge. While the jetlike particle pair density is narrowly confined, the ridge is broadly distributed and is approximately uniform in $\Delta\eta$. A Gaussian fit in R to the average correlated pair density of the ridge yields $\sigma > 1.48$ with 84% confidence level. Unlike the correlation between particles in $\Delta\phi \sim 0$, the particles from the ridge appear to be uncorrelated in $\Delta\eta$ not only with the trigger particle, but also between themselves; they are uniform in our measured $\Delta\eta$ range event by event. No correlation is found between production of the ridge and production of the jetlike particles, suggesting the ridge may be formed from the bulk medium itself.

We thank the RHIC Operations Group and RCF at BNL, the NERSC Center at LBNL and the Open Science Grid consortium for providing resources and support. This work was supported in part by the Offices of NP and HEP within the U.S. DOE Office of Science, the U.S. NSF, the Sloan Foundation, the DFG cluster of excellence "Origin and Structure of the Universe", CNRS/IN2P3, STFC and

EPSRC of the United Kingdom, FAPESP CNPq of Brazil, Ministry of Ed. and Sci. of the Russian Federation, NNSFC, CAS, MoST, and MoE of China, GA and MSMT of the Czech Republic, FOM and NWO of the Netherlands, DAE, DST, and CSIR of India, Polish Ministry of Sci. and Higher Ed., Korea Research Foundation, Ministry of Sci., Ed. and Sports of the Rep. Of Croatia, Russian Ministry of Sci. and Tech, and RosAtom of Russia.

*Deceased.

[1] J. Adams *et al.* (STAR Collaboration), Phys. Rev. Lett. **95**, 152301 (2005).
[2] B. I. Abelev *et al.* (STAR Collaboration), Phys. Rev. C **80**, 064912 (2009).
[3] N. Armesto, C. A. Salgado, and U. A. Wiedemann, Phys. Rev. Lett. **93**, 242301 (2004).
[4] A. Majumder, B. Müller, and S. A. Bass, Phys. Rev. Lett. **99**, 042301 (2007).
[5] C. B. Chiu and R. C. Hwa, Phys. Rev. C **72**, 034903 (2005).
[6] C. Y. Wong, Phys. Rev. C **78**, 064905 (2008).
[7] S. A. Voloshin, Phys. Lett. B **632**, 490 (2006).
[8] E. Shuryak, Phys. Rev. C **76**, 047901 (2007).
[9] A. Dumitru *et al.*, Nucl. Phys. **A810**, 91 (2008).
[10] K. Dusling *et al.*, Nucl. Phys. **A828**, 161 (2009).
[11] J. Takahashi *et al.*, Phys. Rev. Lett. **103**, 242301 (2009).
[12] K. H. Ackermann *et al.* (STAR Collaboration), Nucl. Instrum. Methods Phys. Res., Sect. A **499**, 624 (2003).
[13] B. I. Abelev *et al.* (STAR Collaboration), Phys. Rev. Lett. **102**, 052302 (2009).
[14] K. H. Ackermann *et al.* (STAR Collaboration), Nucl. Phys. **A661**, 681 (1999).
[15] J. Adams *et al.* (STAR Collaboration), Phys. Rev. C **72**, 014904 (2005).
[16] J. G. Ulery and F. Wang, Nucl. Instrum. Methods Phys. Res., Sect. A **595**, 502 (2008).
[17] P. Abreu *et al.*, Phys. Lett. B **407**, 174 (1997).
[18] T. Sjöstrand *et al.*, Comput. Phys. Commun. **135**, 238 (2001).
[19] M. M. Aggarwal *et al.* (STAR Collaboration), arXiv:1004.2377.
[20] A. Feng (STAR Collaboration), J. Phys. G **35**, 104082 (2008).